Case B: Estimating economic costs of admissible carbon dioxide reduction paths on a regional level

Abstract

In this paper, we model and forecast carbon dioxide emissions for eight global regions: North, South and Central America, Europe, Africa, Asia, Oceania, and the Middle East. Our model is a region-level vector-error-correction model. We then assign carbon dioxide reduction paths to the different regions that would allow future paths of global hemispheric carbon dioxide concentration to be aligned with the four Representative Concentration Pathways (RCPs) outlined by the Intergovernmental Panel on Climate Change (IPCC). In the second part of the paper, we shift our focus to the interaction between economy and climate. In order to do so, we focus on the United States of America (US), and simulate economic activity in the US under different scenarios of carbon dioxide emission reduction. Our model suggests an increase of real GDP by 7.5% and an increase of industrial production by 3% towards 2100 under RCP2.6. In contrary, our model predict real GDP to increase by 45% and industrial production to increase by 43% towards 2100 under RCP8.5.

This version: April 12, 2019

I. Introduction

Much of the focus in both the academic and political debates about climate change has evolved around greenhouse gases like methan or carbon dioxide. Greenhouse gases are a class of chemical objects that are associated with the greenhouse effect of climate change: anthropogenically emissions of such gases increase their concentration level in the atmosphere and disrupt the earth's energy balance by reflecting some of the energy back to the earth's surface that otherwise would be emitted into space. Among greenhouse gases, carbon dioxide (CO_2) is notoriously famous because it is particularly reflective. The reason is that carbon dioxide's eigenmodes - the frequency at which carbon dioxide molecules start to resonate, thus to take up and send back energy - is approximately the same as the frequency with which the earth surface reflects energy back to the atmosphere. With increasing levels of CO_2 concentration, more energy will be reflected back to the earth surface, and vice versa, leading to a feedback mechanism: climate change.

In the first part of the paper, we propose to model the carbon emissions from eight different regions through a Vector Error-Correction Model (VECM). First, we estimate the model using emission time series from the eight world regions. Equipped with the model coefficients, we recursively forecast regional emissions one-year-ahead from 2018 to 2100. We then study the implications of the four RCP scenarios and compute by how much each region should reduce its CO_2 emission to jointly reach the four global levels of carbon dioxide concentration of the four RCP scenarios. We then propose a distribution scheme for the required emission reductions across regions, in which each country should reduce its CO_2 emission based on its fraction of forecasted emissions.

In the second part of the paper, we shift our focus to the interaction between economy and climate. To do so, we focus on one individual country, the United States of America (US), and forecast the response of economic activity in the US under the four scenarios. We explore how US-macroeconomic variables, Gross Domestic Product (GDP) and Industry Production (IP), would evolve under carbon dioxide concentration pathways that correspond to the four RCP scenarios. Our model suggests an increase of real GDP by 7.5% and an increase of industrial production by 3 % towards 2100 under RCP2.6. In contrary, our model predict real

GDP to increase by 45% and industrial production to increase by 43% towards 2100 under RCP8.5.

II. Data and Descriptives

A. Sample Selection and Data Aggregation

The included data-series used in the empirical part of this paper are obtained from several sources. The Geographical levels of fuel-based carbon dioxide emission are based on the United Nations Framework Convention on Climate Change (short UNFCCC) (June 2017) and the Carbon Dioxide Information Analysis Center (CDIAC). We aggregate the carbon dioxide emission data for eight geographical regions: North, Central and South America, Europe, Asia, Oceania, the Middle East and Africa.[1]

We use global hemispheric carbon dioxide concentration forecasts from our solution of the first part of the first paper of the Econometric Game 2019 that built on four time series of carbon dioxide flow variables: the carbon dioxide emission from fossil fuels, E^{FF}, the carbon dioxide emission from changes in land-use, E^{LUC}, the carbon dioxide sink rate of the ocean, S^{OCN}, and the land sink rate S^{LND}. All time series cover the time period 1959 to 2017.

In the second part of this paper, we consider the relationship between carbon dioxide emission and economic activity in the US. Based on this, we will examine how the required emission reduction that lead to the RCP CO_2 concentration scenarios affect the economic activity in the US based on the real GDP in 2012 levels and industrial production with base level 2017.

B. Properties of the Geographical Carbon Dioxide Emission Time Series

Figure 1 shows the time series of fuel-based carbon dioxide emission and their first differences for the eight geographic regions from 1959 to 2017. Asia, Europe and North America show the highest emissions of carbon dioxide to the atmosphere. Starting in the late 1990s, the Asian countries overtook Europe

[1] A list of which countries are part of each region can be found on: `https://cdiac.ess-dive.lbl.gov/ftp/ndp030/regional_definitions.txt`.

and North America as the world's most carbon dioxide emitting region - a trend that had started in the late 1960s and is probably related to the fast pace of industrialization particularly in China that set in during the late 1970s. This can also be seen by the large increase in the first difference of the series, plotted in the lower part of the figure. The other geographic regions still play a minor role in global carbon dioxide production. Whereas Europe's and North America's absolute CO_2 emission has been slightly decreasing since the early 2000s, all other geographic regions seem to have increased their carbon dioxide emission over the last fifty years.

Figure 1: Time Series and First Differences of Carbon Dioxide Emission by different Regions.

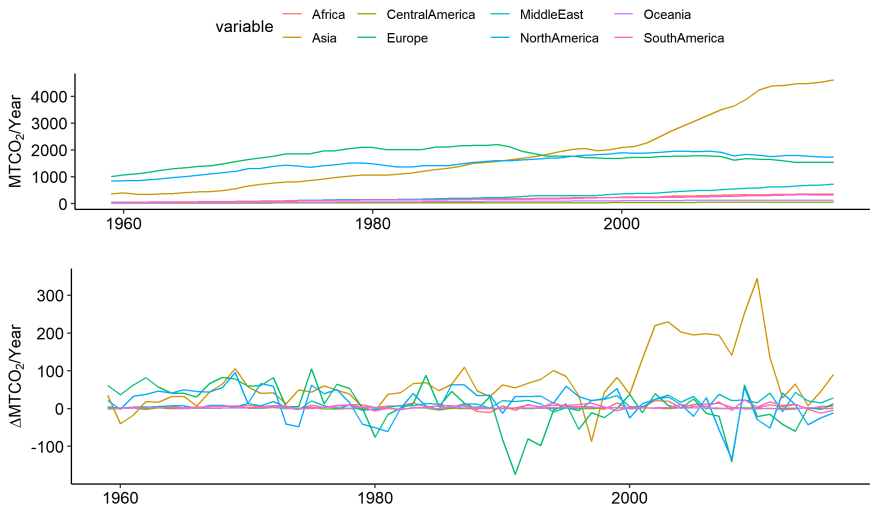

For each of the eight considered carbon series, we test for unit roots using the Augmented Dickey-Fuller (ADF) test (for more details on the test see Fuller (2009)). The ADF-test tests the null hypothesis that there is a unit root in the process against the alternative that the process is stationary. It relies on estimating the following regression equation

$$\Delta y_t = \alpha + \beta t + \gamma y_{t-1} + \delta_1 \Delta y_{t-1} + \cdots + \delta_p y_{t-p} + \varepsilon_t, \tag{1}$$

and testing for a unit root is equivalent to testing $\gamma = 0$. We consider various versions of the test based on whether the model includes a constant ($\alpha \neq 0$) and/or trend ($\beta \neq 0$) and provide the summary statistic of the tests in the Appendix. A

robust finding across all specifications (excluding a constant and a trend and different amount of lags) is that we cannot reject the null hypothesis of a unit root on any conventional significance level. As a further robustness test, we test for unit roots using the MacKinnon (1996) test and the Perron (1988) test and obtain the same conclusion. We conclude therefore that all processes contain a stochastic trend. In order to test for a common stochastic trend we also use the Johansen test for cointegration (see Johansen (1988)). By this, we can test for different numbers of cointegration relationships sequentially using the trace test and the long run Vector Error Correction Model (VECM) formulation (more details on the VECM is provided in Section A below). The null hypothesis of the tests is the presence of $r < k$ cointegration relationships against the alternative that $r = k$ and so the test is done sequentially for $r = 0, 1, \ldots, 7$ (as we have eight time series). We consider different lag length for robustness. We reject the null of no cointegration relationship for all lag length between one and four. Depending on the exact number of lags used in the model, the number of cointegration relationships vary between between four and six.

III. Econometric Models

Based on the presence of unit roots and cointegration relationships in the considered time-series, we choose a model that is able to take those time-series properties into account. We use a VECM which is designed to capture long-run relationships among nonstationary time series. The advantage of VECMs compared to simpler unconstrained models is that they may provide a better understanding of the interaction of different series, which, under correct specification, can lead to improved forecasting performance.

A. Vector Error Correction Model

Let $Y_t = (\text{Africa}_t, \text{Asia}_t, \ldots, \text{SouthAmerica}_t)$ be the vector of climate variables. The classical classical vector autoregressive (VAR) model, which lays the foundation for the VECM used bewlow, is given by

$$\Theta(L)Y_t = \delta + \epsilon_t, t \in 1, \ldots, n, \tag{2}$$

where $\Theta(L)$ is a $k \times k$ matrix lag polynomial of degree p

$$\Theta(L) = I_k - \Theta_1 L - \cdots - \Theta_p L^p, \tag{3}$$

δ is a $p \times 1$ vector of intercepts, and ϵ_t is a $p \times 1$ vector of weakly stationary and serially uncorrelated white noise error terms. In order to take the cointegration relationship into account, we extend to a VECM given by

$$\Delta Y_t = \mu + \Pi Y_{t-p} + \Gamma_{p-1} \Delta Y_{t-p+1} + \cdots + \Gamma_1 \Delta Y_{t-1} + \varepsilon_t, \tag{4}$$

which is basically a VAR model specified in first-differences, which includes the long-run relationship of Y_t determined by the $p \times p$ matrix Π. Further, μ is a $p \times 1$ vector of intercepts and Γ_i is the $p \times p$ vector autoregressive parts. Choosing the model specification amounts to choosing the number of lags p and the number of cointegration relationships. The latter can be chosen by performing the Johansen test (testing the rank of Π) sequentially.

Under quadratic loss the optimal forecast of the VECM is the relevant conditional expectation. The optimal forecast for y_T made at time T for time $T+h$ is therefore simply obtained as a recursive one-step ahead forecasts according to

$$\hat{y}_{T+h|T} = \mathbb{E}\left[\hat{y}_{T+h} \mid \hat{y}_{T+h-1|T}, \hat{y}_{T+h-2|T}, \ldots\right]. \tag{5}$$

B. VECM specification comparison

In order to select the preferred VECM specification we examine the in-sample data fit for different lag lengths and various cointegration relationships. We start with the usual information criteria, which are depicted in Table 1. Whereas the AIC favors the model with two lags and one cointegration relationship, BIC prefers the specification with two lags and four cointegration relationships. Next, we explore the in-sample root mean-squared-error (RMSE) obtained from the fitted values based on the different VECM specifications and the actual values. The results are shown in Table 2. They show that the specification with two lags and one cointegration relationship has the lowest RMSEs, which is also the favored AIC-based model.

Table 1: Information criteria

p	r	AIC	BIC
1	1	2056.958	2218.359
1	2	2025.792	2213.753
1	3	1992.925	2203.359
1	4	1974.503	2203.325
1	5	1964.999	2208.122
2	1	2015.381	2305.007
2	2	1962.699	2278.654
2	3	1936.311	2274.545
2	4	1917.719	2274.181
2	5	1906.260	2276.899

This table shows information criteria for different VECM specifications.

Next, we investigate the out-of-sample performance of the various models under consideration and whether the superiority of the model with two lags and one cointegration relationship carries over to reliable out-of-sample forecast accuracy. We split the data set into an estimation and evaluation sample. The in-sample data covers the period 1959 through 2000, and the remaining sample is kept to examine the accuracy of the forecast. Based on the recursive forecasting approach depicted in Section A we forecast future paths of the variables and compute the RMSE for each of the series and for each models. The results are provided in Table 2. The best out-of sample fit is provided by the specification with one lag and one cointegrating relationship. Hence, in order to avoid issues arising from overfitting, we will in what follows, continue with the specification based on the best out-of-sample performance and refrain from the more complicated specification which showed the best in-sample fit. Henceforth, we will thus refer to the specification with one lag and one cointegration relationship as the preferred VECM specification.

Table 2: In-sample RMSE

p	r	Africa	Asia	Cent-Am	Europe	MidEast	N-Am	Oceania	S-Am	AveRMSE
1	1	24.292	129.755	2.779	122.628	18.522	275.859	5.362	21.601	75.100
1	2	25.423	167.249	2.501	135.422	20.057	260.223	5.656	15.193	78.966
1	3	16.367	76.302	2.502	138.278	25.072	240.742	4.465	13.265	64.624
1	4	15.942	80.636	3.199	138.979	19.193	201.931	2.931	16.428	59.905
1	5	13.176	78.967	2.936	143.059	28.956	193.483	2.844	19.066	60.311
2	1	14.359	105.612	2.763	196.457	17.362	184.919	4.575	19.304	68.169
2	2	14.905	88.373	3.442	102.040	17.099	181.886	4.268	17.906	53.740
2	3	14.950	88.434	3.451	97.112	13.469	180.140	4.236	18.129	52.490
2	4	12.936	106.905	2.105	96.713	13.527	187.067	3.453	17.718	55.053
2	5	13.729	102.160	2.048	103.216	16.119	158.448	1.993	19.954	52.208

The table shows the in-sample RMSE of different VECM specifications for the different global regions.

Table 3: Out-of-sample RMSE

p	r	Africa	Asia	Cent-Am	Europe	MidEast	N-Am	Oceania	S-Am	AveRMSE
1	1	8.353	97.895	1.683	68.889	18.972	70.463	2.823	8.532	34.701
1	2	10.286	104.527	2.027	72.393	19.392	70.600	2.798	8.898	36.365
1	3	10.701	89.734	2.201	68.675	19.962	71.410	2.943	8.883	34.314
1	4	11.291	91.572	2.117	68.929	21.051	71.116	2.634	9.801	34.814
1	5	10.888	91.626	2.265	68.999	21.717	71.607	2.599	10.077	34.972
2	1	13.148	87.049	2.937	90.021	20.801	86.652	3.297	9.499	39.175
2	2	12.137	82.041	2.789	84.754	25.200	90.346	2.928	10.475	38.834
2	3	13.024	81.795	2.983	94.566	26.185	101.351	3.398	10.867	41.771
2	4	14.243	82.669	2.746	91.697	27.010	98.880	3.612	10.840	41.462
2	5	14.368	82.834	2.706	85.968	28.352	97.813	3.361	11.355	40.844

The table shows the out-of-sample RMSE of different VECM specifications for the different global regions.

IV. Results

The following section collects the results of our study. In Section A, we present the parameter estimates of our preferred VECM. Then, we continue with a richer discussion of the in- and out-of-sample fit of the preferred VECM specification in Section B, where we in the latter use the VECM to forecast carbon dioxide emission paths for the eight geographic regions. Section C discusses how we link fuel-based carbon dioxide emission to the overall change in hemispheric carbon dioxide emission. In Section D, we finally conduct policy scenarios for the eight geographical regions based on the different RCPs.

A. VECM Parameter Estimates

The estimated parameter values of of the preferred VECM specification are depicted in Table 4. In general, the CO_2 emission of a given region loads significantly

on its own lagged emission value and the error correction term (ECT). That is, after taking the cointegration relationship into account the estimated parameter value of the cross-lags appear mostly insignificant and the emission of a given region does not add further explanation power for future emission of a different geographic regions. However, some significant cross region effects does exist, such as between ('L.' denotes the lagged value of a given region) Africa and L.Asia, Europe and L.Africa, Europe and L.SouthAmerica, MiddleEast and L.Asia, MiddleEast and L.Europe, Oceania and L.CentralAmerica, Oceania and L.NorthAmerica, SouthAmerica and L.Asia, SouthAmerica and L.Europe and SouthAmerica and L.MiddleEast. These relationship might correspond to an effect of trade between the different region, i.e., if Europe has a high emission from increased production (an expanding economy), trade with South America might increase, prompting their emission to increase.

B. Model Fit and Forecasting

To check the performance of our model, we investigate how our fitted series relate to the observed series of carbon emission for each of the eight regions considered. The results are illustrated in Figure 2. In general, the model perform well with only a few and small deviations from the observed series. An exception is North America where the fitted series seems to be somewhat below the actual series. Next, we present the out-of-sample forecasting results for each of the eight regions. Using the specified model, we perform a recursive forecast of both the yearly emission in million ton carbon and the regional stock in ppm. Note that the stock is the forecasted ppm which each of the regions are responsible for and does not relate to the stock of carbon dioxide in a spatial sense. Figure 3 shows the forecasted flows, and shows that the individual series converge quickly to their stable long-run values, which is a theoretical feature of the VECM and corresponds to when the dynamic system of series attain their long-run equilibrium. This holds also for the the forecasted stocks illustrated in Figure 4. In the long run, the forecasts converge to a constant increase in carbon for each period, implying a continuously increasing stock of carbon.

Table 4: Parameter estimates of the preferred VECM specification

	$\hat{\beta}$	s.e.($\hat{\beta}$)	t-stat($\hat{\beta}$)	p-value
Africa:ECT	0.243	0.082	2.957	0.005
Africa:Africa-1	-0.150	0.182	-0.825	0.414
Africa:Asia-1	0.044	0.012	3.718	0.001
Africa:CentralAmerica-1	0.311	0.646	0.482	0.632
Africa:Europe-1	-0.023	0.017	-1.347	0.184
Africa:MiddleEast-1	-0.115	0.077	-1.504	0.139
Africa:NorthAmerica-1	0.009	0.023	0.377	0.708
Africa:Oceania-1	0.228	0.460	0.495	0.623
Africa:SouthAmerica-1	-0.109	0.151	-0.721	0.475
Asia:ECT	0.524	0.765	0.686	0.496
Asia:Africa-1	-1.472	1.694	-0.869	0.389
Asia:Asia-1	0.791	0.110	7.178	0.000
Asia:CentralAmerica-1	4.912	6.012	0.817	0.418
Asia:Europe-1	-0.049	0.157	-0.312	0.757
Asia:MiddleEast-1	0.367	0.714	0.513	0.610
Asia:NorthAmerica-1	-0.180	0.218	-0.827	0.413
Asia:Oceania-1	4.021	4.286	0.938	0.353
Asia:SouthAmerica-1	0.074	1.407	0.053	0.958
CentralAmerica:ECT	0.059	0.020	3.046	0.004
CentralAmerica:Africa-1	-0.049	0.043	-1.144	0.258
CentralAmerica:Asia-1	0.003	0.003	1.086	0.283
CentralAmerica:CentralAmerica-1	-0.308	0.153	-2.008	0.050
CentralAmerica:Europe-1	-0.006	0.004	-1.485	0.144
CentralAmerica:MiddleEast-1	0.024	0.018	1.299	0.200
CentralAmerica:NorthAmerica-1	0.007	0.006	1.288	0.204
CentralAmerica:Oceania-1	-0.097	0.109	-0.885	0.380
CentralAmerica:SouthAmerica-1	-0.032	0.036	-0.890	0.378
Europe:ECT	2.409	0.600	4.017	0.000
Europe:Africa-1	-2.688	1.328	-2.023	0.049
Europe:Asia-1	0.088	0.086	1.020	0.313
Europe:CentralAmerica-1	-3.474	4.714	-0.737	0.465
Europe:Europe-1	0.336	0.123	2.727	0.009
Europe:MiddleEast-1	-0.379	0.560	-0.677	0.502
Europe:NorthAmerica-1	0.025	0.171	0.148	0.883
Europe:Oceania-1	0.287	3.360	0.086	0.932
Europe:SouthAmerica-1	-3.686	1.103	-3.341	0.002
MiddleEast:ECT	0.524	0.164	3.201	0.002
MiddleEast:Africa-1	-0.604	0.362	-1.666	0.102
MiddleEast:Asia-1	0.099	0.024	4.223	0.000
MiddleEast:CentralAmerica-1	-0.208	1.286	-0.162	0.872
MiddleEast:Europe-1	-0.090	0.034	-2.666	0.010
MiddleEast:MiddleEast-1	0.023	0.153	0.151	0.881
MiddleEast:NorthAmerica-1	0.042	0.047	0.894	0.376
MiddleEast:Oceania-1	0.169	0.917	0.184	0.855
MiddleEast:SouthAmerica-1	-0.301	0.301	-1.001	0.322
NorthAmerica:ECT	0.344	0.594	0.580	0.565
NorthAmerica:Africa-1	-0.914	1.316	-0.694	0.491
NorthAmerica:Asia-1	-0.009	0.086	-0.107	0.915
NorthAmerica:CentralAmerica-1	-6.375	4.671	-1.365	0.179
NorthAmerica:Europe-1	0.007	0.122	0.055	0.956
NorthAmerica:MiddleEast-1	0.423	0.555	0.761	0.450
NorthAmerica:NorthAmerica-1	0.394	0.169	2.332	0.024
NorthAmerica:Oceania-1	4.507	3.329	1.354	0.182
NorthAmerica:SouthAmerica-1	-0.880	1.093	-0.805	0.425
Oceania:ECT	0.097	0.019	5.075	0.000
Oceania:Africa-1	-0.025	0.042	-0.604	0.549
Oceania:Asia-1	0.002	0.003	0.672	0.505
Oceania:CentralAmerica-1	-0.313	0.150	-2.092	0.042
Oceania:Europe-1	-0.006	0.004	-1.635	0.109
Oceania:MiddleEast-1	0.022	0.018	1.250	0.217
Oceania:NorthAmerica-1	0.018	0.005	3.419	0.001
Oceania:Oceania-1	0.056	0.107	0.529	0.599
Oceania:SouthAmerica-1	-0.064	0.035	-1.816	0.076
SouthAmerica:ECT	0.170	0.073	2.330	0.024
SouthAmerica:Africa-1	-0.098	0.162	-0.604	0.549
SouthAmerica:Asia-1	0.047	0.011	4.508	0.000
SouthAmerica:CentralAmerica-1	-0.566	0.574	-0.986	0.329
SouthAmerica:Europe-1	-0.040	0.015	-2.681	0.010
SouthAmerica:MiddleEast-1	-0.143	0.068	-2.099	0.041
SouthAmerica:NorthAmerica-1	0.031	0.021	1.488	0.143
SouthAmerica:Oceania-1	0.114	0.409	0.279	0.782
SouthAmerica:SouthAmerica-1	0.072	0.134	0.533	0.596

This tables shows the estimated parameter values for the preferred VECM specification with one lag and one cointegration relationship together with its standard errors, t-statistics, and p-value.

Figure 2: In-Sample Model Fit Flow.

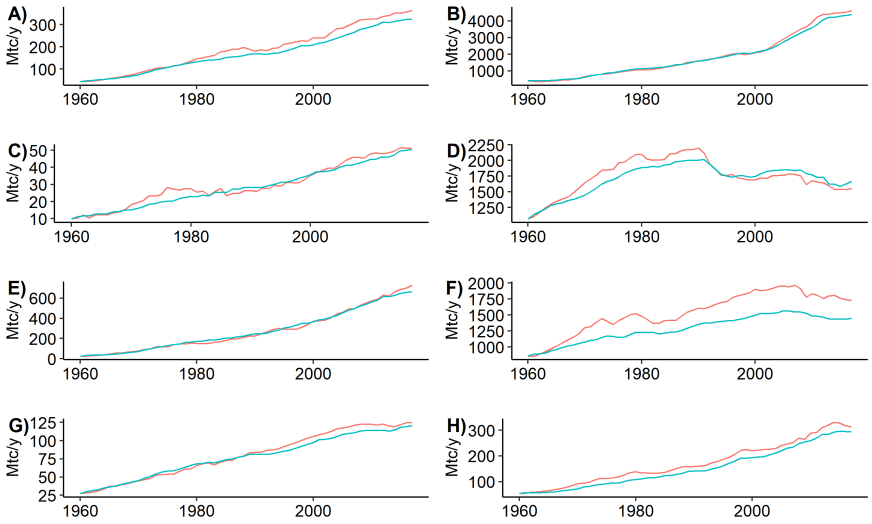

The figure illustrates the in-sample model fit of our preferred VECM of the hemispheric carbon dioxide flow in the different geographic regions. The actual data points are coloured in red and the fitted values in blue. The geographical regions are, reading from left to right and starting from subplot A: Africa, Asia, Central America, Europe, Middle East, North America, Oceania and South America.

Figure 3: Forecasting carbon dioxide emission for different world Regions

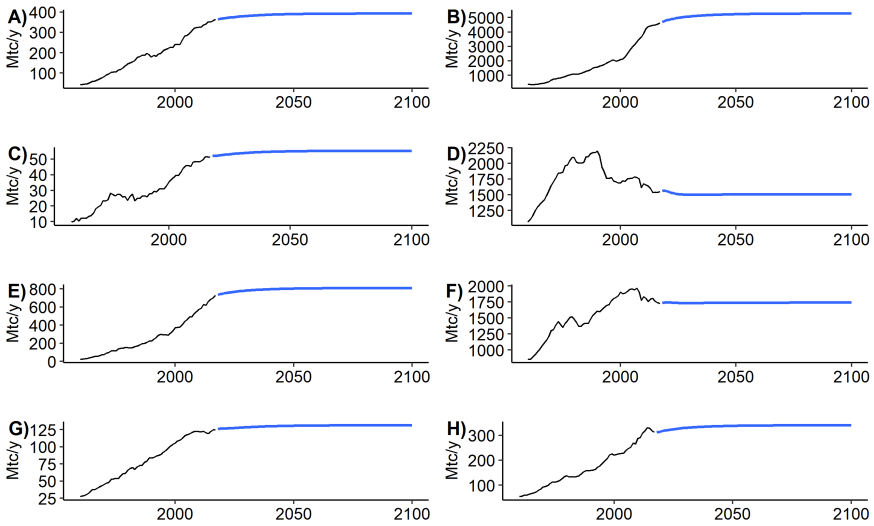

The figure plots recursive forecasts of carbon dioxide emission for different world regions based on our preferred VECM specification. The geographical regions are, in clockwise order and starting from subplot A: Africa, Asia, Central America, Europe, Middle East, North America, Oceania and South America.

Figure 4: Forecasting stocks of carbon dioxide for different world Regions

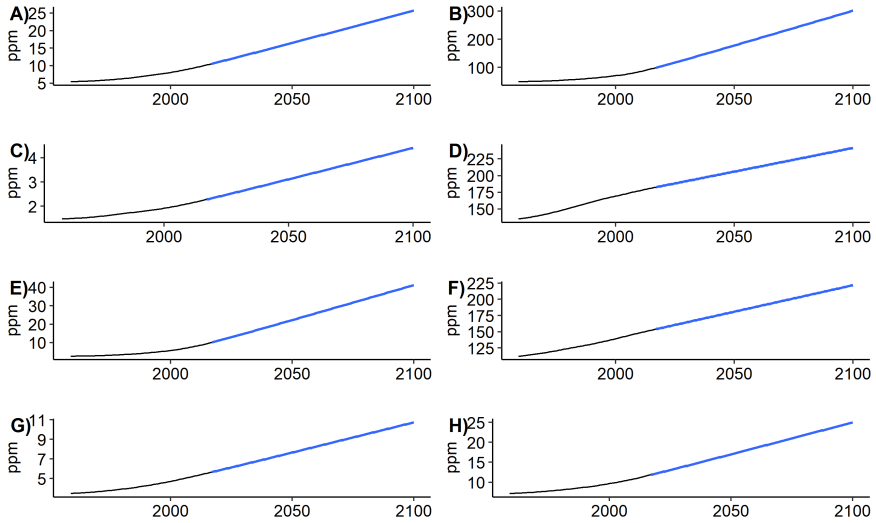

The figure plots recursive forecasts of hemispheric carbon dioxide concentration for different world regions based on our preferred VEC model specification. The geographical regions are, reading from left to right and starting from subplot A: Africa, Asia, Central America, Europe, Middle East, North America, Oceania and South America.

C. Linking Region-Level Emission to the Global RCP transmission paths

Linking regional-level carbon dioxide emission forecasts to the global RCP carbon dioxide concentration scenarios is not a trivial undertaking, because the stock of global hemispheric carbon dioxide is mediated by the global carbon budget, while the basis of our analysis are regional fuel-based carbon dioxide emissions.

We therefore need to link changes in the atmospheric carbon dioxide level to fuel based greenhouse gas emissions of every individual geographic regions. We do so by referring to our global carbon dioxide concentration forecast from case A and extrapolate from our individual regional-level fuel-based carbon dioxide forecasts in the following way. Consider the global carbon budget equation:

$$G_t^{AMT} = E_t^{LUC} + E_t^{FF} - S_t^{LND} - S_t^{OCN} \tag{6}$$

where $E_t^{ANT} = E_t^{LUC} + E_t^{FF}$ is anthropologically released CO_2 into the atmosphere, where E_t^{LUC} are carbon dioxide emissions from changes in land-use and E_t^{FF} fuel-

based carbon dioxide emissions, G_t^{AMT} is the growth of atmospheric CO_2 emission, S_t^{LND} is the exchange flow of CO_2 from atmosphere and hydrosphere (the land sink) and S_t^{OCN} is the flow of CO_2 from atmosphere to biosphere (the ocean sink). For each geographical region $r \in R$, we now approximate its contribution to global carbon dioxide mission in year t as:

$$G_{r,t}^{AMT} = \frac{E_{r,t}^{FF}}{\sum_{r \in R} E_{r,t}^{FF}} \cdot G_t^{AMT} \tag{7}$$

where we replace G^{AMT} with the forecasted values from case A, $\hat{G}^{AMT}$, and E_r^{FF} with the forecasted values from Section B, $\hat{E}_r^{FF}$.

D. Policy Analysis

In this part of the paper, we analyse different policies that aim at reducing carbon dioxide emissions on a global level so that the RCP carbon dioxide concentration goals can be reached. However, as the data we use for the analysis is emissions, i.e. flows of carbon, we need to change this into the corresponding stocks for each region. Using the same fraction as we used in (7), we calculate the stock in ppm for each region in 1959 by:

$$ppm_{r,1959} = \frac{E_{r,t}^{FF}}{\sum_{r \in R} E_{r,t}^{FF}} \cdot ppm_{1959} \tag{8}$$

and then calculate the path for each region using the observed values. For out-of-sample forecast, each of the values in (8) is replaced with its predicted value. Figure 5 shows the result of this. For each region, we show the forecasted emission path with no change is made, along with the four different RCPs. Our model predicts that the emission will be very close to the level corresponding to RCP6 (the blue line).

Figure 5: Forecasted Carbon Dioxide Emission Scenarios for the different Regions

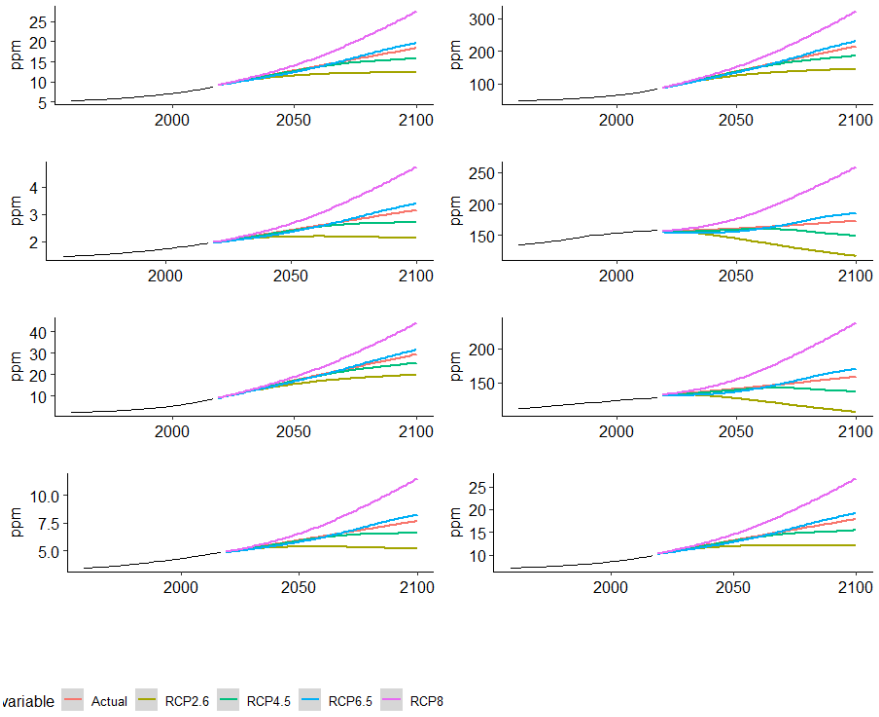

The graph plots forecasted scenarios for the different geographic regions. Our forecast from the first case of the econometric games 2019 is coloured in ... The geographical regions are, reading from left to right: Africa, Asia, Central America, Europe, Middle East, North America, Oceania and South America.

We next consider the necessary emission reductions necessary to arrive at the different goals. To do this, we first calculate the percentage difference between the forecasted emission level and the one necessary to achieve the different RCP levels for each region and multiply it with the its forecasted atmospheric carbon flow:

$$PD_{r,t} = \frac{ppm_{r,t} - ppm_{RCP,t}}{ppm_{r,t}} \cdot G^{AMT}_{r,t} \tag{9}$$

The result is plotted in Figure 6. As can be seen from the plot, the yearly emissions have be increasingly reduced moving towards 2100. The increase happens because each region is forecasted to increase its emission. For the industrialized regions, we see that the emissions have to be reduced by a lot in order to comply with the best or second best RCP. Specifically, we forecast that the Asian region have

to reduce its reduction by a approximately 1000 Mtc/year in 2100 in order to comply with the best RCP. The European and North American region are second in how much should be reduced with a approximately 500 Mtc/year reduction necessary in 2100. The necessary reduction for the remaining region is more conservative corresponding to their relatively small part in the global emission budget. The negative reductions corresponding to RCP6 and RCP8.5 for the different regions happens because they are forecasted to end below the level of these RCPs, meaning that emission can actually be increased in order to reach this level.

However, it is not immediately clear how these necessary reductions to reach the more ambitious levels are going to affect the economic activity of the regions. In the following section, we try to answer this by looking at the relationship between the economy and the carbon emission, focusing on the US.

Figure 6: Reduction Paths for Different World Regions

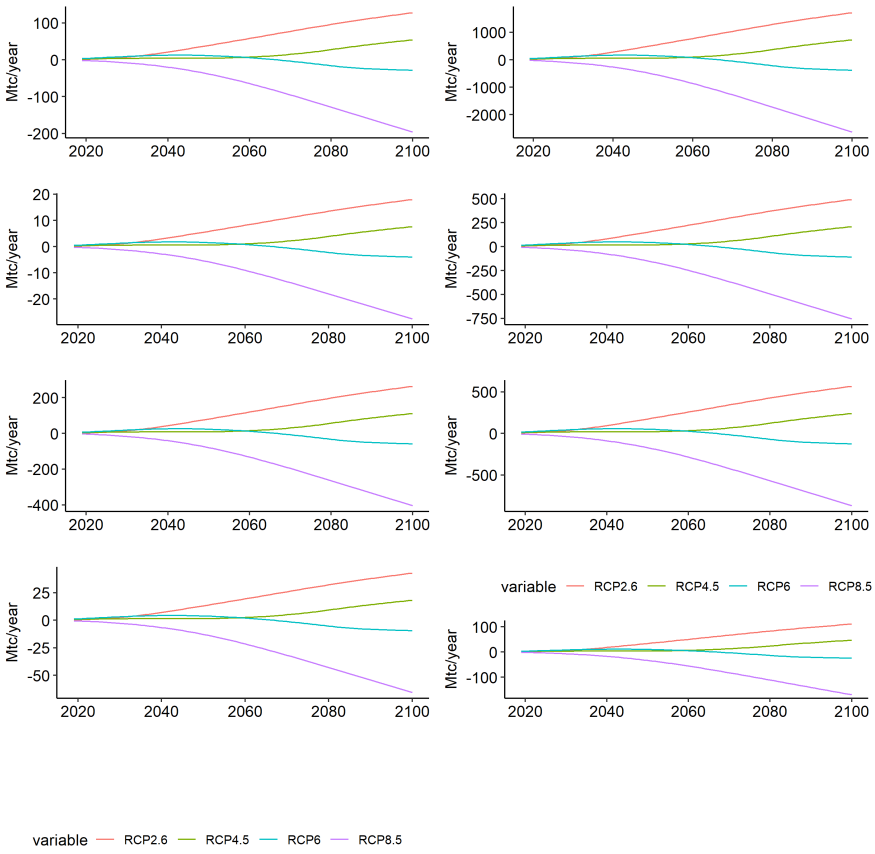

The graph plots reduction paths for the eight world regions that would guarantee to achieve the different global hemispheric carbon trajectories from the RCP's. The geographical regions are, reading from left to right: Africa, Asia, Central America, Europe, Middle East, North America, Oceania and South America.

V. Global Carbon Emission and Economic Activity: The Case of the US

Up until now, we considered carbon dioxide emission reductions without explicitly taking the economy into account. In this section, we take a closer look at the interaction between the climate and the economy. We narrow our focus on the US, mainly because the US economy is the world's largest and because it produces a large share of the yearly global carbon dioxide emission.

Our strategy is to extend the region-level VECM to capture a connection between the emissions of a region and broad economic indicators, and in particular, we focus on Gross Domesti Product (GDP) and Industry Production (IP). That is, we specify a region-level VECM as before but include times series of GDP and IP. We refer to the model as the region-level, economy-augmented VECM. Then, we feed the pathways of US emissions that correspond to the RCP scenarios into the region-level, economy-augmented VECM and explore what the required emission reductions imply for the GDP and IP, respectively. That is, based on the time series of regional emissions in 1959-2017, the times of real GDP and IP in 1959-2017, and the estimated model coefficients, we forecast real GDP and IP from 2018-2100 based on the four different RCP scenarios.

A. Specification of the Economy-Augmented VECM

To find the optimal specification of the model, we consider a set of combinations of lag length $p \in \{1,2\}$ and cointegration relationships $r \in \{1,2,3,4,5\}$. This amounts to ten different specification, which we compare based on AIC, BIC, in-sample RMSE, and out-of-sample RMSE.

Table 5: Information criteria of different specifications

p	r	AIC	BIC
1	1	2596.347	2839.470
1	2	2555.307	2833.162
1	3	2523.019	2831.519
1	4	2492.977	2828.037
1	5	2475.804	2833.338
2	1	2524.451	2968.003
2	2	2458.491	2936.474
2	3	2415.898	2924.261
2	4	2384.691	2919.384
2	5	2357.912	2914.883

This table shows the AIC and BIC for ten different model specifications.

From Table 5, we see that the specification with $p = 2$ and $r = 5$ is best in terms of

AIC, whereas the specification with $p = 1$ and $r = 4$ is best according to the BIC. In Table 6, we report the in-sample RMSE, where the lowest average RMSE is obtained for $p = 2$ and $r = 5$ in line with the AIC.

Table 6: In-Sample RMSE for different specifications

p	r	Africa	Asia	Cent-Am	Europe	Mid-East	N-Am	Oceania	S-Am	GDP	IP	AveRMSE
1	1	29.527	111.041	3.371	164.948	16.093	243.583	4.929	39.616	805.014	14.477	143.260
1	2	30.118	153.697	2.868	149.366	16.664	241.832	4.743	37.237	847.116	14.949	149.859
1	3	27.247	129.112	2.826	189.446	29.570	268.408	3.731	29.179	892.187	17.369	158.907
1	4	26.589	108.391	2.773	138.160	28.940	281.168	3.772	27.050	934.899	18.018	156.976
1	5	26.095	107.567	2.543	138.347	23.816	277.720	3.472	28.272	965.334	18.632	159.180
2	1	25.402	70.283	3.090	143.261	15.040	245.357	5.399	25.747	955.802	13.152	150.253
2	2	23.841	63.574	1.933	109.789	20.815	221.193	5.219	23.864	945.103	12.127	142.746
2	3	14.454	88.017	3.561	70.805	23.352	174.770	1.458	17.065	572.886	9.348	97.572
2	4	15.392	86.925	2.481	65.162	14.278	180.240	1.384	16.442	538.013	9.174	92.949
2	5	14.863	64.770	1.925	63.733	14.499	121.191	1.434	11.221	202.264	2.452	49.835

This table shows the in-sample RMSE for ten different model specifications. The model that obtains the lowest in-sample RMSE uses a specification of $p = 2$ and $r = 5$.

Finally, we re-do the out-of-sample exercise, in which we estimate the model using data up until 2000 and then recursively compute out-of-sample one-step-ahead forecasts up until 2017. The RMSE from this exercise is reported in Table 7, and shows that the lowest average RMSE is obtained for $p = 1$ and $r = 2$. This indicates that the favored models based on the three in-sample criteria AIC, BIC, and in-sample RMSE might suffer from overfitting. That is, the specification that obtains the lowest out-of-sample RMSE is simpler than the preferred in-sample model specification. Consequently, as we mainly care about out-of-sample forecasting performance, we proceed with specifying a VECM with lag length $p = 1$ and 2 cointegration relationships.

Table 7: Out-of-Sample RMSE of the Augmented VECM

p	r	Africa	Asia	Cent-Am	Europe	Mid-East	N-Am	Oceania	S-Am	GDP	IP	AveRMSE
1	1	7.011	92.099	1.812	72.610	17.790	66.305	2.646	10.509	306.133	5.256	58.217
1	2	7.720	80.736	2.107	81.636	19.260	68.768	2.586	10.659	299.948	5.398	57.882
1	3	7.785	82.863	2.041	76.520	20.648	72.247	2.500	10.476	315.501	5.620	59.620
1	4	9.496	83.509	2.294	81.794	20.550	69.934	2.400	10.546	321.951	5.466	60.794
1	5	10.042	82.149	2.431	82.334	20.503	74.004	2.641	11.418	337.001	5.900	62.842
2	1	12.494	70.764	3.119	108.306	26.628	90.247	2.686	11.155	351.815	5.868	68.308
2	2	15.964	62.908	3.532	107.887	25.894	107.812	3.315	11.894	458.820	6.621	80.465
2	3	15.307	57.658	3.549	98.049	32.510	105.539	3.319	12.139	451.081	6.537	78.569
2	4	16.547	56.243	3.396	88.926	28.870	107.480	3.207	13.507	442.705	6.623	76.750
2	5	16.019	58.052	3.354	92.022	29.164	115.537	3.579	14.328	548.905	7.795	88.875

This table shows the out-of-sample RMSE for ten different model specifications. The model that obtains the lowest out-of-sample RMSE uses a specification of $p = 1$ and $r = 2$.

B. Forecasting Economic Activity in the US under different CO_2 emission scenarios

We now turn to forecasting broad economy indicators under different RCP scenarios based on our preferred economy-augmented VECM specification. We estimate the model coefficients based on the regional emissions time series as well and the GDP and IP time series for the period 1959-2017. Having estimated the model, we conduct a counterfactual analysis, in which we explore how the GDP and IP would evolve under the four RCP scenarios. More specifically, we fix four pathways for US emissions according to the RCP scenarios. Given each of the scenarios, we recursively forecast the remaining regional emissions as well as the GDP and IP for the US. By this, we take the cointegration relationships into account as those were estimated without fixing the US emission time series. The results from the counterfactual analysis are shown in Figure 7.

Figure 7: Trajectories of economic indicators under different RCP scenarios

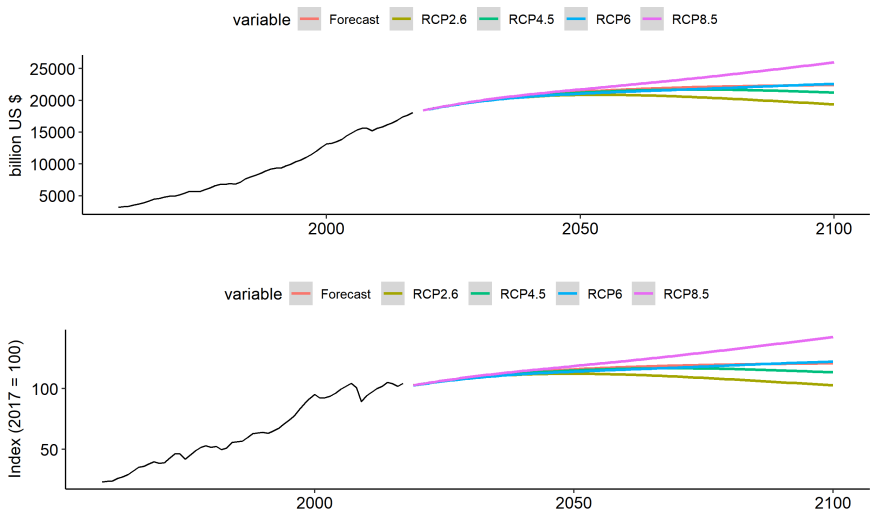

The figure illustrates the implications of required emission reductions for the GDP (top) and IP (bottom) given the region-level, economy-augmented VECM. In the RCP2.6 scenario, the model suggests that both GDP and IP increase slightly in the long run. In the RCP8.5 scenario, the suggests that both GDP and IP increases more substantially in the long run. The model forecasts coincide with the RCP6 scenario.

First, we consider the top panel, which shows the actual and forecasted real GDP in 2012 levels under the different RCP scenarios. In 2100, the forecasted real GDP ranges from 19,400 billion USD under RCP2.6 to 26,000 billion USD under

RCP8.5. In 2017, the real GDP in 2012 levels was 18,000 billion USD. Thus, the forecasts correspond roughly to an increase of 7.5% under RCP2.6 and an increase of 45% under RCP8.5 in 2100. The benchmark forecast of real GDP, in which we do not fix the US emissions, coincides with the RCP6 scenario. Turning to IP, we consider the bottom panel of Figure 7. Under RCP2.6, our model suggests that IP increases roughly 3% towards 2100, i.e. the IP index is forecasted to increase from index 100 in 2017 to index 102.8 in 2100. On the contrary, the IP is expected to increase by roughly 43% towards 2100 under the RCP8.5 scenario.

VI. Conclusion

In the first part of the paper, we propose to model the carbon emissions from regions by a VECM as this is able to capture long-run equilibrium relationships among non-stationary time series. First, we estimate the model using emission time series from the eight world regions. Equipped with the model coefficients, we forecast recursively regional emissions one-year-ahead from 2018 to 2100. We then study the implications of the four RCP scenarios and compute by how much each region should reduce its CO_2 emission to jointly reach the four RCP scenarios. We propose a distribution scheme for the required emission reductions across regions, in which each country should reduce its CO_2 emission based on its fraction of forecasted emissions. That is, if a global emission reduction is required of 5 GtC in a given year, say 2050, to comply with RCP2.6 and North America is responsible for 20% of the total emissions in the same year, then our model suggests a distribution scheme in which North America should reduce its emission in 2050 by 1 GtC.

In the second part of the paper, we extend our model to a region-level, economy-augmented VECM. This extension takes the real GDP in 2012 levels and the industrial production index with base year 2017 into account. Again, we estimate the model parameters during the period 1959-2017, in which period we include all eight emission time series in addition to the two time series of the real GDP and IP index. Then, we use the required emission paths for North America under the four different RCP scenarios and feed these trajectories into the estimated model and forecast the remaining seven regional emissions and economic indicators from 2018 to 2100. The two most extreme RCP scenarios, namely RCP2.6 and

RCP8.5, imply very different economic conditions in 2100. Under the RCP2.6 scenario, the real GDP is forecasted to increase by roughly 7.5% from 2017 to 2100, and the IP is forecasted to increase by roughly 3%. In contrast, under the RCP8.5 scenario, our model predicts an increase in real GDP by 45% towards 2100, and an increase in IP by 43% towards 2100.

However, we suggest to approach our results with great caution. Forecasting as far into the future as the year 2100 is not a trivial thing to do; economists regularly fail in predicting the state of the economy only a very few years ahead. Forecasting carbon dioxide emission broadly shares some key features of the main difficulties in macroeconomic forecasting.

A first problem of our estimates is the small number of data points. In the climate science and climate econometric literature, researchers are e.g. struggling to reconcile how the decrease in global surface temperature between 1996 and 2008 matches the evidence of anthropologically caused climate change (Kaufmann, Kauppi, Mann, and Stock (2011)). Having longer time series would clearly facilitate the detection of long climatic cycles that could otherwise be missclassified as structural breaks in climate models.

Furthermore, we do not take the endogeneity of carbon dioxide emission and economic activity into account. Economic activity increases atmospheric greenhouse gas concentration, with different effects on global and regional climates. When facing economic damages from climate change, the economy is expected to respond by adapting its production structure in the long run. Pretis (2017) hints at this problem and stresses that the climate econometric literature suffers from plausibly unreasonable exogeneity assumptions on the interaction between the climate and the economy. He argues that one strand of the literature takes the economy as fixed and models climate change as a response to given economic activity (e.g. Kaufmann et al. (2011) or Estrada, Perron, and Martínez-López (2013)), while another stresses human and social responses to climate change (see Dell, Jones, and Olken (2014), Jones and Olken (2010)). The models and forecasts in our paper are in the spirit of the first fixed-economy literature, as we do not properly consider endogenous feedback mechanism between climate change and human behavior. For instance, our model assumes that the economic

policy is stable. If political organizations e.g. decided to drastically tax carbon dioxide emission, economic theory predicts that the economy should substitute away from carbon dioxide based economic activity.

Last, our forecasts neglect the role of economic innovation. Nordhaus (2010) argues that neglecting economic innovation will most likely lead to overestimates of climate change, but admits that the economic profession has little sense of the magnitude of the bias. In particular in the context of the US, it could very well be the case that ambitious carbon dioxide reduction programs or high carbon taxes might foster innovation in carbon-free energy production, with potential positive spillovers to the entire globe.

References

DELL, M., B. F. JONES, AND B. A. OLKEN (2014): "What do we learn from the weather? The new climate-economy literature," *Journal of Economic Literature*, 52, 740–98.

ESTRADA, F., P. PERRON, AND B. MARTÍNEZ-LÓPEZ (2013): "Statistically derived contributions of diverse human influences to twentieth-century temperature changes," *Nature Geoscience*, 6, 1050.

FULLER, W. A. (2009): *Introduction to statistical time series*, vol. 428, John Wiley & Sons.

JOHANSEN, S. (1988): "Statistical analysis of cointegration vectors," *Journal of economic dynamics and control*, 12, 231–254.

JONES, B. F. AND B. A. OLKEN (2010): "Climate shocks and exports," *American Economic Review*, 100, 454–59.

KAUFMANN, R. K., H. KAUPPI, M. L. MANN, AND J. H. STOCK (2011): "Reconciling anthropogenic climate change with observed temperature 1998–2008," *Proceedings of the National Academy of Sciences*, 108, 11790–11793.

MACKINNON, J. G. (1996): "Numerical distribution functions for unit root and cointegration tests," *Journal of applied econometrics*, 11, 601–618.

NORDHAUS, W. D. (2010): "Modeling induced innovation in climate-change policy," in *Technological change and the environment*, Routledge, 188–215.

PERRON, P. (1988): "Trends and random walks in macroeconomic time series: Further evidence from a new approach," *Journal of economic dynamics and control*, 12, 297–332.

PRETIS, F. (2017): "Exogeneity in climate econometrics," .

A. Appendix

Table 8: Augmented Dickey Fuller test for unit root

Table 9

lag	ADF_1	p.value	ADF_2	p.value	ADF_3	p.value
0	6.594	0.990	0.942	0.990	-1.978	0.576
1	4.367	0.990	0.827	0.990	-1.953	0.586
2	3.037	0.990	0.574	0.987	-2.048	0.547
3	2.346	0.990	0.382	0.979	-2.082	0.533
0	9.207	0.990	4.258	0.990	-0.432	0.982
1	2.169	0.990	1.106	0.990	-1.463	0.789
2	2.602	0.990	1.380	0.990	-0.837	0.953
3	1.326	0.951	0.423	0.981	-1.525	0.764
0	3.348	0.990	0.093	0.961	-1.706	0.688
1	3.554	0.990	0.032	0.956	-1.358	0.832
2	3.326	0.990	0.095	0.961	-1.191	0.901
3	1.922	0.985	-0.143	0.937	-1.749	0.671
0	0.811	0.872	-2.975	0.046	-2.123	0.516
1	0.272	0.718	-2.324	0.205	-2.045	0.548
2	0.074	0.662	-2.398	0.177	-2.279	0.454
3	-0.020	0.635	-2.291	0.217	-2.267	0.458
0	9.472	0.990	4.384	0.990	0.363	0.990
1	6.955	0.990	4.670	0.990	0.696	0.990
2	4.388	0.990	3.526	0.990	0.570	0.990
3	4.064	0.990	3.610	0.990	0.877	0.990
0	2.138	0.990	-2.778	0.073	-0.406	0.983
1	1.324	0.951	-2.436	0.162	-0.917	0.943
2	1.287	0.948	-2.749	0.077	-0.931	0.941
3	0.556	0.799	-2.443	0.159	-1.540	0.757
0	6.333	0.990	-1.218	0.617	-0.773	0.959
1	3.608	0.990	-1.226	0.614	-0.826	0.954
2	2.518	0.990	-1.362	0.567	-0.891	0.947
3	1.805	0.980	-1.424	0.545	-1.309	0.853
0	5.411	0.990	0.730	0.990	-1.862	0.624
1	3.318	0.990	0.360	0.978	-2.032	0.554
2	1.333	0.952	-0.477	0.877	-2.855	0.227
3	1.982	0.987	0.235	0.972	−2.332	0.433 height

This table shows the result from running the augmented Dickey Fuller test for unit root on all the region specific time series. The three test are for a model with no trend nor constant, a model with just a constant and a model with constant and trend. Reading from the top, we the time series is for region: Africa, Asia, Central America, Europe, Middle East, North America, Oceania and South America.